17th World Conference on Earthquake Engineering, 17WCEE
Sendai, Japan - September 13th to 18th 2020

STATIC CYCLIC LOADING TEST OF LIGHT GAUGE STEEL AND LIGHTWEIGHT CONCRETE SHEAR WALLS

C. Quan[(1)], Q. Huang[(2)], D. Li[(3)], Y. Chen[(4)]

[(1)] *Assistant professor, Osaka institute of technology, chunri.quan@oit.ac.jp*
[(2)] *Chief director, China BIM union, hqianghq@cbtgc.com*
[(3)] *Chief engineer, China building technique group co., ltd., lidongbin@cbtgc.com*
[(4)] *Engineer, ARSE building engineering technology co., ltd., chenyong20130709@163.com*

Abstract

Cold-formed steel structure has been widely used in the low-rise buildings due to its high strength, ease of construction and low cost. On the other hand, due to low self-weight, good workability, excellent performance on thermal insulation and sound absorption, lightweight concrete is primarily utilized as non- or semi-structural material in the building construction.

This paper presents a new structure system named light gauge steel and lightweight concrete (LSLC) structure, which used expanded polystyrene concrete or foamed concrete as structural material in composite way with cold-formed steel. Here, the shear walls are the main structural members for the LSLC structure system, which are assembled with the light gauge steel lattice columns and horizontal braces, and filled with lightweight concrete (Fig. 1). The lattice columns are composed of two or four steel tubes, which are combined and fixed by batten plates and bolts. Steel strips with W-shaped cross section are installed as horizontal braces, which are connected to the lattice columns by self-drilling screws.

In order to grasp the seismic performance of the LSLC shear walls, several specimens with different shear span ratio and axial force ratio as the experimental parameters are tested under the static cyclic lateral loading. This paper describes the design details and testing method for the LSLC shear wall specimens. Then, the damage state and hysteresis loops of specimens are presented detailly. Finally, the effects of shear span ratio and axial force ratio on seismic capacity of the LSLC shear walls, such as horizontal load bearing capacity and deformation capacity, are discussed based on the test results.

As a result, the LSLC structure shows the possibility to become a construction option of low-rise or mid-rise buildings in the seismic region. And, these research results should be become valuable basis for the design standard establishment of the LSLC structure system.

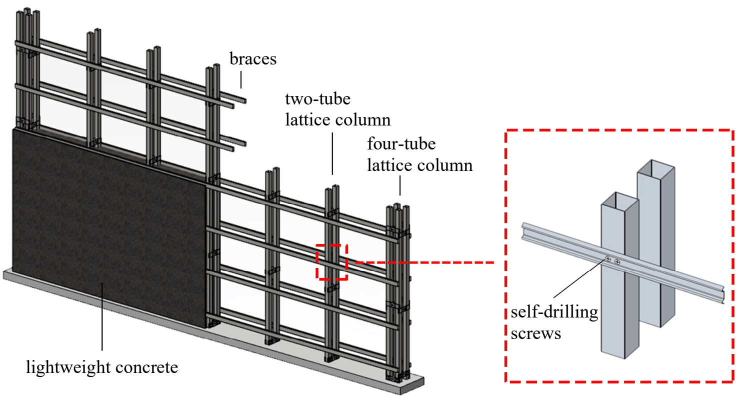

Fig. 1 – Configuration of the LSLC shear wall

Keywords: light gauge steel and lightweight concrete structure, shear wall, seismic capacity, static cyclic loading test

1. Introduction

Cold-formed steel (CFS) structure has been widely used in the low-rise buildings due to its high strength, ease of construction, and low cost [1-6]. On the other hand, due to low self-weight, good workability, excellent performance on thermal insulation, fire resistance and sound absorption, lightweight concrete was primarily utilized as non- and semi-structural material in the past building construction [7-11]. Motivated by the industrialized performance of CFS structure, good integrity of cast-in-situ concrete structure and advantages of the lightweight concrete, a new structure system named light gauge steel and lightweight concrete (LSLC) structure, which used expanded polystyrene concrete or foamed concrete as the structural material in composite way with the cold-formed steel, was proposed and applied to the building construction in China [12]. Compared with the traditional reinforced concrete structure, the LSLC structure can reduce seismic load significantly based on the use of lightweight concrete to decrease the self-weight of overall structure. Compared with the CFS structure, the LSLC structure has great advantages in features such as fire protection, thermal insulation and sound absorption.

In the past several years, the studies of the LSLC structure were focused on the members such as shear walls and slabs, furthermore their design method has been developed based on the considerable tests. This paper describes the design details and testing method for the LSLC shear wall specimens, with different shear span ratio and axial force ratio as the experimental parameters. Then, the damage state and hysteresis loops of specimens are presented detailly based on the static cyclic lateral loading test results. Finally, the effects of shear span ratio and axial force ratio on seismic capacity of the LSLC shear walls, such as lateral load bearing capacity and deformation capacity are discussed.

2. Outline of experiment

2.1 Configuration of the LSLC shear wall

Shear wall is the main structural member of the LSLC structure system. Fig. 1 shows the standard configuration of the shear wall with thickness of 180mm and concrete cover thickness of 20mm. Light gauge steel frame is assembled with the light gauge steel lattice columns and horizontal braces, then filled with lightweight concrete. The lattice columns composed of two or four square steel tubes, which were combined and fixed by batten plates and bolts with 600 mm spacing as shown in Fig. 2. Steel strips with W-shaped cross section were installed as horizontal braces with spacing of 600mm, which were connected to the lattice columns by self-drilling screws.

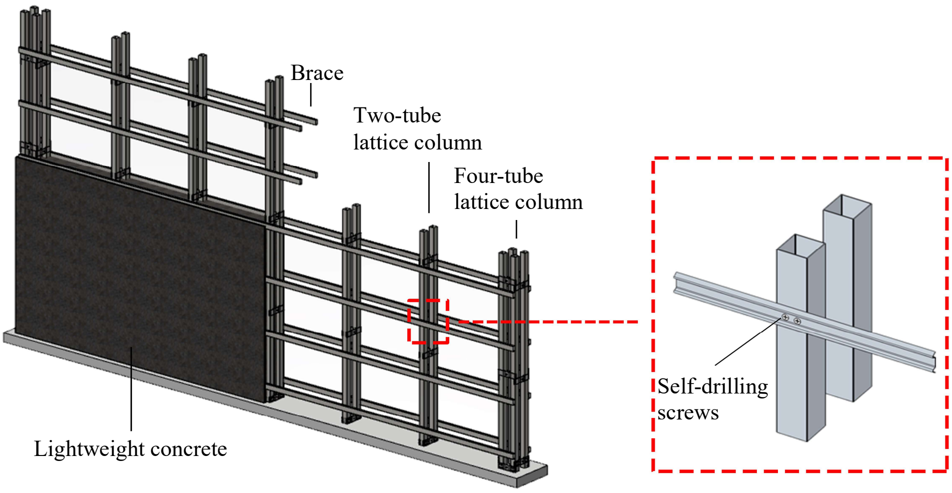

Fig. 1 – Configuration of the LSLC shear wall

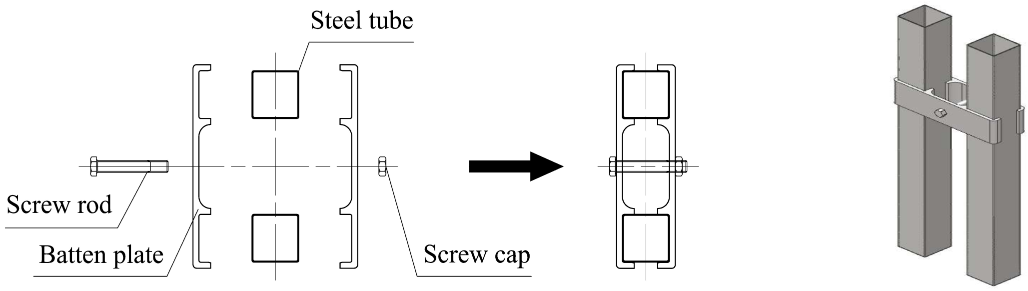

(a) Top view (b) 3D graph

Fig. 2 – Installation of batten plates in the lattice column

2.2 Design of specimen

The test specimens are designed according to the standard design method of LSLC shear wall mentioned above. In this study, five full-scale specimens with different shear span ratio and axial force ratio as the experimental parameters are tested under in-plain cyclic loadings.

Table 1 and Fig. 3 show the experiment parameters and design details of specimens. The light gauge steel lattice columns of each specimen are composed of four and two square steel tubes at the side and the middle of the wall, respectively. Then, the lattice columns are anchored in the reinforced concrete regid beam (stub). The horizontal braces are installed with spacing of 600mm, which are connected to the lattice columns by three self-drilling screws.

Table 1 – Experiment parameters

Specimen	**Height × Width × Thickness (mm)**	**Shear span ratio**	**Axial force ratio**
S0.8-A0.4	1650 × 2062.5 × 180	0.8	0.4
S1.5-A0.4	2250 × 1500 × 180	1.5	0.4
S2.5-A0.4	2250 × 900 × 180	2.5	0.4
S1.5-A0.2	2250 × 1500 × 180	1.5	0.2
S1.5-A0.3	2250 × 1500 × 180	1.5	0.3

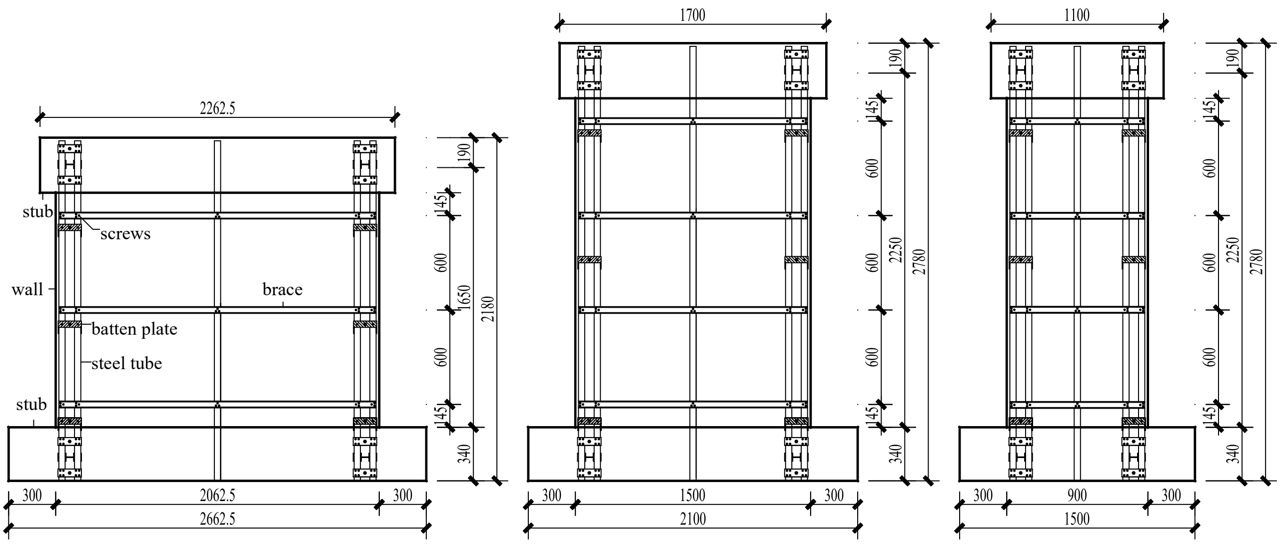

(a) S0.8-A0.4 specimen (b) S1.5-A0.2/0.3/0.4 specimen (c) S2.5-A0.4 specimen

Fig. 3 – Details of specimens (unit: mm)

Table 2 – Mechanical properties and cross-section size of light gauge steel

Member	Yield strength	Tensile strength	Young's modulus	Cross-section (mm)
Lattice column	361.5 MPa	484.3 MPa	2.02×10^5 MPa	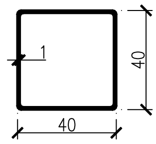
Horizontal brace	352.1 MPa	462.2 MPa	1.98×10^5 MPa	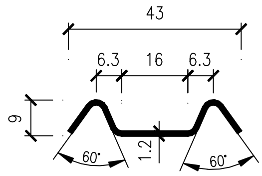

Table 3 – Mechanical properties of lightweight concrete (expanded polystyrene concrete)

Density	Compressive strength	Elastic modulus
1058 kg/m^3	6.36 MPa	0.72×10^4 MPa

2.3 Material characteristic

Tables 2 and 3 show the material test results, where the values represent the mean value of 3 samples in each test. The light gauge steel is designated as S350GD conform to the Chinese National Standard GB/T2518-2008 [13]. which requires the yield strength and tensile strength not less than 350MPa and 420 MPa, respectively. In addition, No.4.8 self-drilling screw given in the ISO15481:1999 [14] is adopted as fastener.

The expanded polystyrene concrete with designing density of 1000kg/m^3 is used as lightweight concrete. Here, test samples with dimensions 100mm×100mm×100mm are prepared in casting process of each specimen, then the compressive strength and density are measured according to the Chinese National Standard GB/T50080-2002 [15].

2.4 Loading program

The loading system and history are shown in Fig. 4 and Fig. 5, respectively. The lateral cyclic loading is performed by load control system until the yielding of light gauge steel. Then, it is switched to displacement control, and peak drift angles (the ratio of lateral deformation to wall height) are planned by the times of displacement (Δ) when the light gauge steel is yielded. Here, two cycles for each peak drift are imposed. The axial load is applied to each specimen based on the axial force ratio.

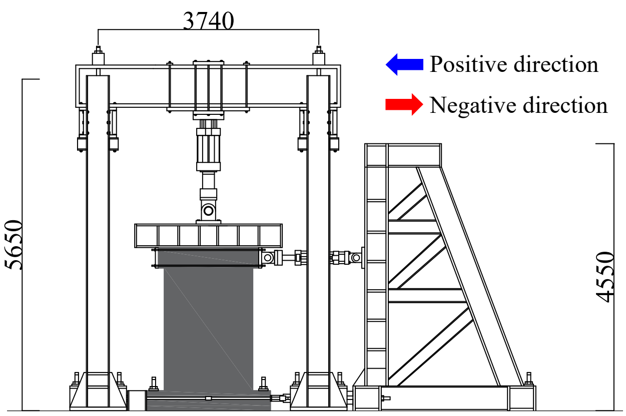

Fig. 4 – Test setup (unit: mm)

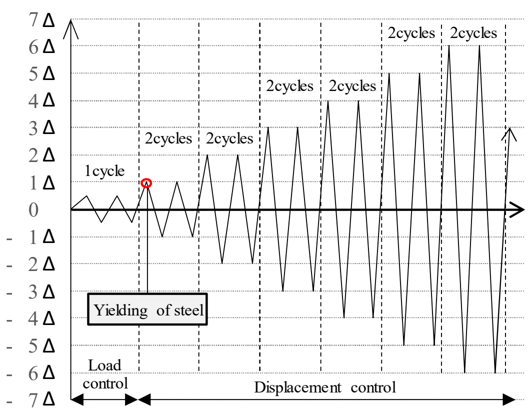

Fig. 5 – Loading history

3. Test results

3.1 Failure patterns

Fig. 6 shows the crack patterns in each specimen at the safety limitation, where it is defined as the moment in which the maximum lateral strength of the LSLC shear wall deteriorates to its 85%.

S0.8-A0.4 specimen: a shear crack at the middle of wall is observed at the drift angle of 0.11% with the width of 0.15mm. Loaded to 0.25%, some vertical cracks occur at the upper of wall along the light gauge steel lattice columns. At the drift angle of 1.88%, clear shear cracks are observed at the diagonal of wall.

S1.5-A0.4 specimen: a shear crack at the bottom of wall is observed at the drift angle of 0.11% with the width of 0.1mm. Loaded to 0.36%, some vertical cracks and flexural cracks occur in succession. At the drift angle of 3.02%, the vertical cracks and flexural cracks continue to extend and the width increases.

S2.5-A0.4 specimen: there are some flexural and flexural-shear cracks are observed at the drift angle of 0.21% with the maximum width of 0.15mm. Loaded to 0.34%, vertical and horizontal cracks occur along the light gauge steel lattice columns and braces. At the drift angle of 3.04%, the width of flexural cracks increases, and local crush of lightweight concrete cover is observed at the bottom of wall.

S1.5-A0.2 specimen: a shear crack at the bottom of wall is observed at the drift angle of 0.07% with the width of 0.05mm. Loaded to 0.17%, some vertical cracks and shear cracks occur at the upper of wall with the maximum width of 0.6mm. At the drift angle of 3.70%, all cracks extend remarkably.

S1.5-A0.3 specimen: a shear crack at the bottom of wall is observed at the drift angle of 0.15% with the width of 0.15mm. Loaded to 0.26%, the width of shear crack increases to 0.8mm, and some vertical cracks occur at the middle of wall. At the drift angle of 3.40%, the vertical cracks and shear cracks continue to extend intensely.

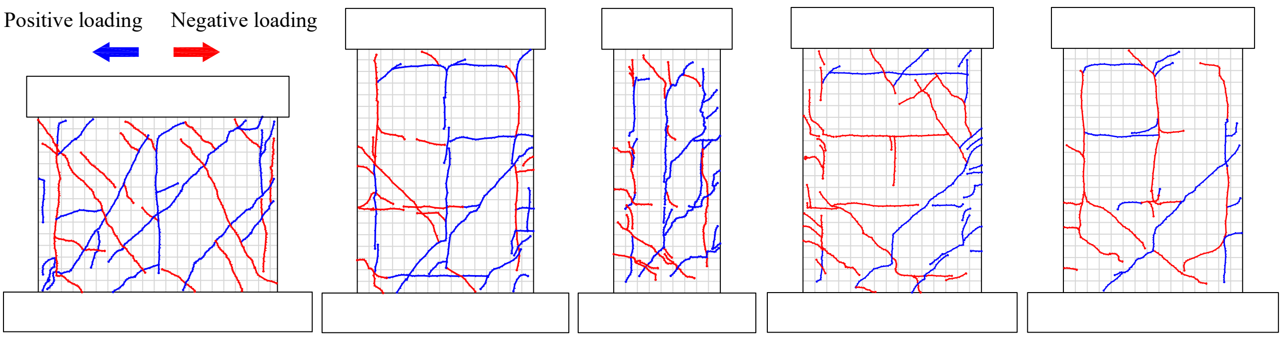

(a) S0.8-A0.4 (b) S1.5-A0.4 (c) S2.5-A0.4 (d) S1.5-A0.2 (e) S1.5-A0.3

Fig. 6 – Crack patterns

3.2 Hysteretic characteristics

Fig. 7 shows the relationship between lateral strength and drift angle.

S0.8-A0.4 specimen: the maximum lateral strength of 295.5kN is recorded at the drift angle of 0.59%. Then, remarkably rapid strength deterioration is observed until the drift angle of 1.53%, which is the safety limitation of the specimen. It shows typical shear failure characteristics.

S1.5-A0.4 specimen: the maximum lateral strength of 146.2kN is recorded at the drift angle of 1.15%. Then, relatively slow strength deterioration is observed until the drift angle of 2.10%, which is the safety limitation of the specimen. It shows flexural-shear failure characteristics.

S2.5-A0.4 specimen: the maximum lateral strength of 73.8kN is recorded at the drift angle of 0.46%. Then, slow strength deterioration is observed until the drift angle of 1.23%, which is the safety limitation of the specimen. It shows typical flexural failure characteristics.

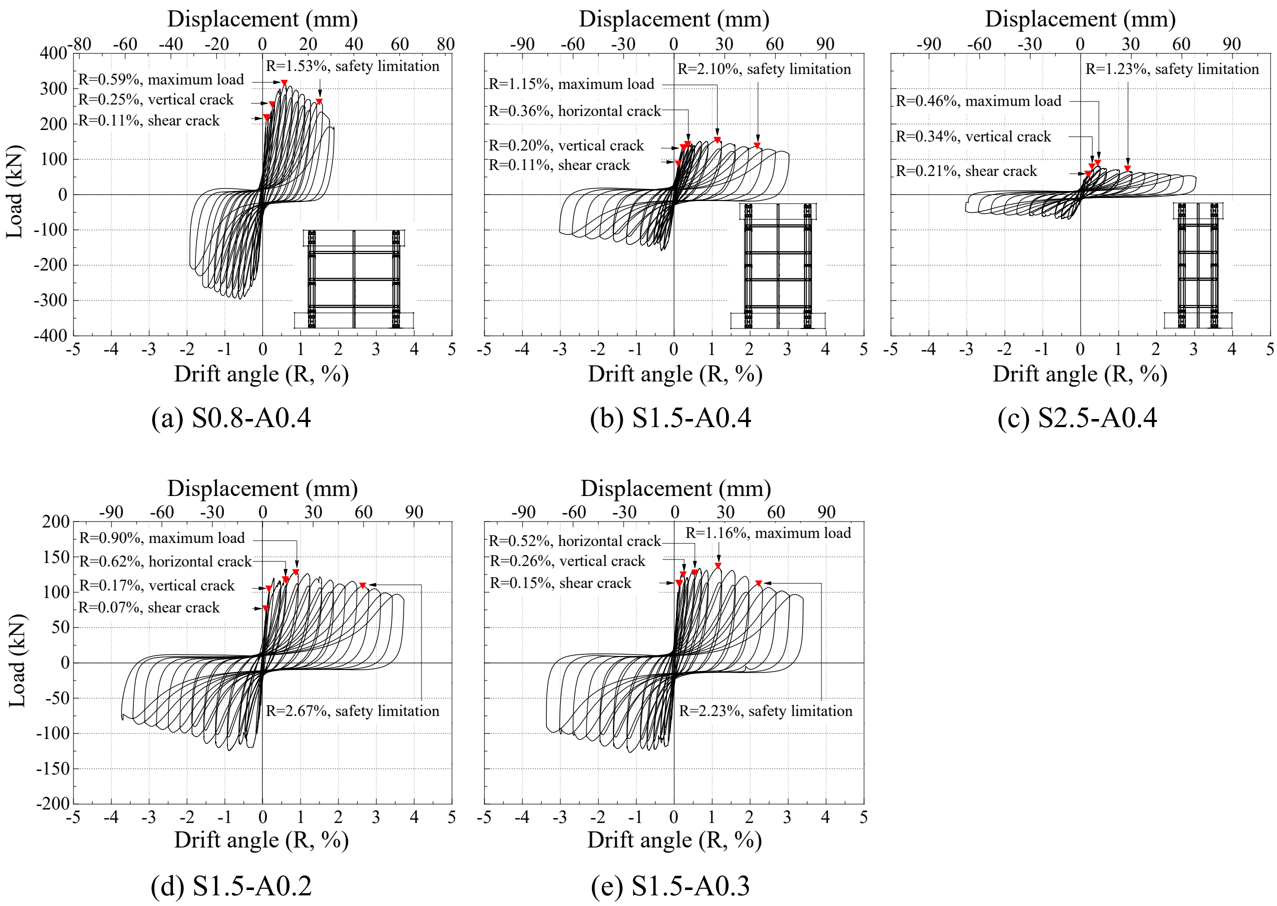

Fig. 7 – Lateral strength and drift angle relation

S1.5-A0.2 specimen: the maximum lateral strength of 121.9kN is recorded at the drift angle of 0.90%. Then, slow strength deterioration is observed until the drift angle of 2.67%, which is the safety limitation of the specimen. It shows flexural-shear failure characteristics.

S1.5-A0.3 specimen: the maximum lateral strength of 124.4kN is recorded at the drift angle of 1.16%. Then, relatively slow strength deterioration is observed until the drift angle of 2.23%, which is the safety limitation of the specimen. It shows flexural-shear failure characteristics.

4. Seismic capacity evaluation

4.1 Lateral load bearing capacity

Fig. 8 shows the relationship between maximum lateral strength and experiment parameters, such as shear span ratio and axial force ratio. The maximum lateral strength decreases with the increase of the shear span ratio (Fig. 8(a)). Compared with the S0.8-A0.4 specimen, the maximum lateral strength of the S2.5-A0.4 specimen decreases by 75.0%. It can be considered that the flexural failure characteristics of shear wall gradually dominates with the increase of the shear span ratio.

The increase of the axial force ratio leads to increase in the maximum lateral strength of the LSLC shear wall (Fig. 8(b)). Compared with the S1.5-A0.2 specimen, the maximum lateral strength of the S1.5-A0.4 specimen increases by 19.9%. It can be considered that the restraint between light gauge steel and lightweight concrete is strengthened under the larger axial force ratio. Also, it is indicated that the effect of shear span ratio and axial force ratio on the lateral load bearing capacity of the LSLC shear wall has the same tendency in the reinforced concrete structure.

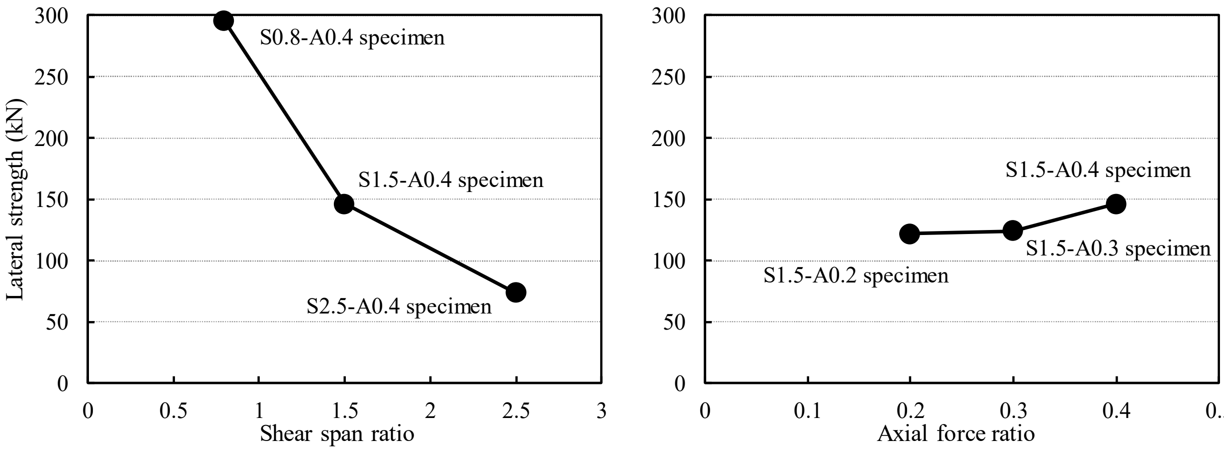

(a) Effect of shear span ratio (b) Effect of axial force ratio

Fig. 8 – Maximum lateral strength of the LSLC shear wall

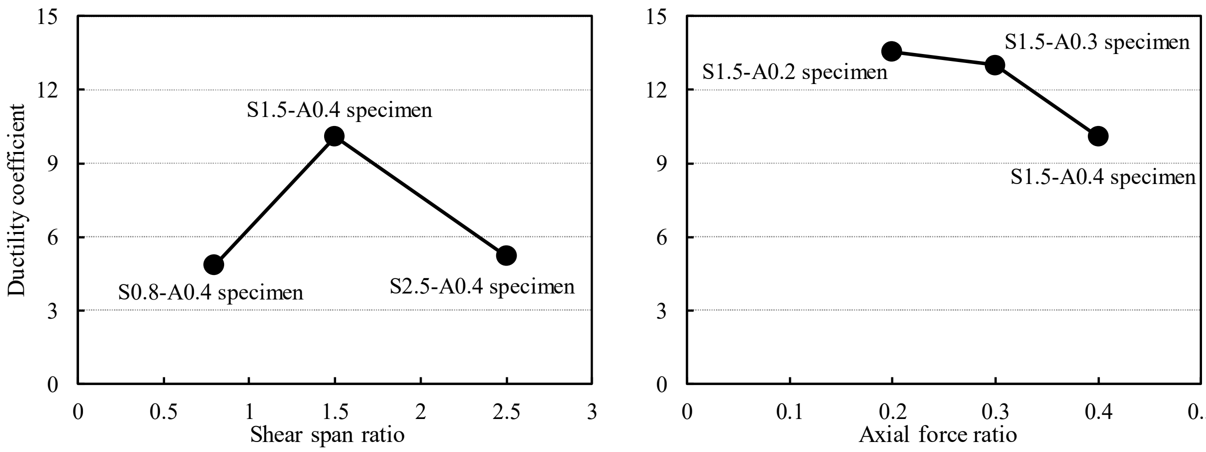

(a) Effect of shear span ratio (b) Effect of axial force ratio

Fig. 9 – Ductility coefficient of the LSLC shear wall

4.2 Deformation capacity

Fig. 9 shows the relationship between ductility coefficient and experiment parameters, such as shear span ratio and axial force ratio. Herein, the ductility coefficient (μ) of the LSLC shear wall is calculated as the ratio of failure displacement (Δ_u, displacement of safety limitation) to yield displacement (Δ_y), which is defined as shown in Fig. 10.

As shown in Fig. 9(a), it is difficult to determine the internal relationship between the shear span ratio and the ductility coefficient of the LSLC shear wall, although the ductility coefficient decreases with the increase of axial force ratio (Fig. 9(b)). And, the ductility coefficient of each specimen is larger than 4, showing better deformation capacity compared with the reinforced concrete shear walls [16].

4.3 Energy absorption capacity

Since the absolute value of dissipated energy depends on the scale of the specimen such as the cross-sectional area, the normalized equivalent damping ratio (h_{eq}) is applied to evaluate the energy absorption capacity of the LSLC shear wall. Herein, the equivalent damping ratio is calculated from the energy absorbed in one cycle ($\varDelta W$) and equivalent potential energy (W_e, strain energy) as shown in Fig. 11.

Fig. 12 shows equivalent damping ratio of each specimen. The maximum value of the equivalent damping ratio for each specimen is recorded 17.19~19.62%. After loading to the drift angle of 0.5%, the equivalent damping ratio of the LSLC shear wall shows the relatively stable values as 12~20%. Compared with the reinforced concrete shear walls [17], the LSLC shear walls show lower energy absorption capacity in this experimental study, and it can be considered that the severe slip of the LSLC shear wall reduced the hysteretic dissipated energy.

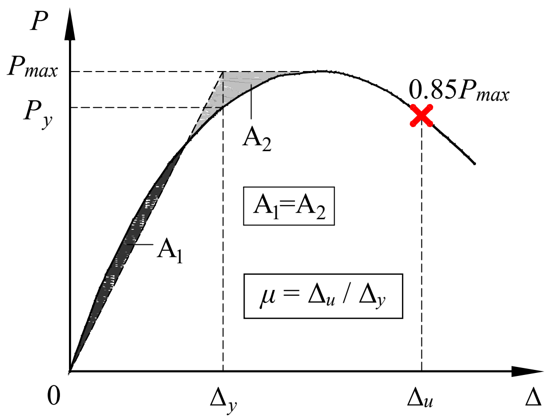

Fig. 10 – Characteristic points of P-Δ curve

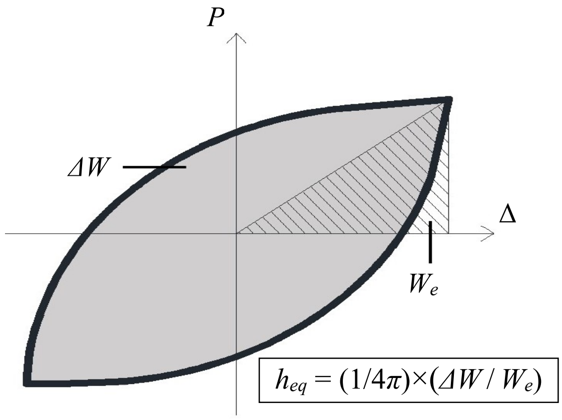

Fig. 11 – Definition of equivalent damping ratio

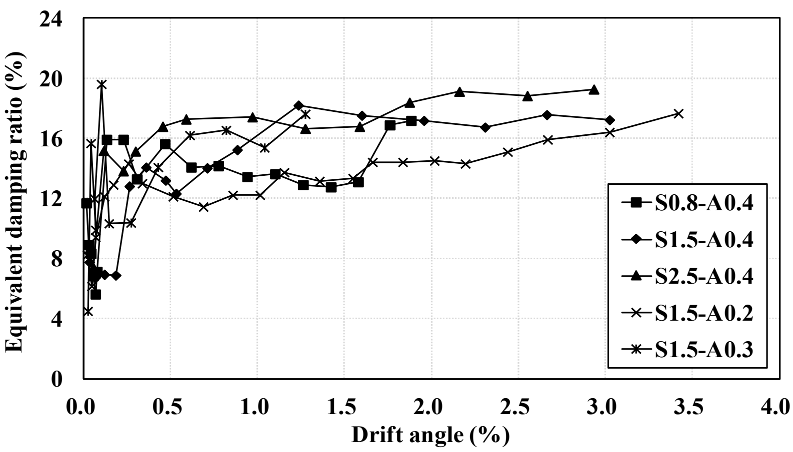

Fig. 12 – Equivalent damping ratio of the LSLC shear wall

5. Conclusions

Seismic performance of the light gauge steel and lightweight concrete shear wall was experimentally investigated under in-plane cyclic loadings. The major findings can be summarized as follows.

(1) The effects of shear span ratio and axial force ratio on the lateral load bearing capacity of the LSLC shear wall are grasped quantitatively.

(2) The ductility coefficient (μ) of each specimen is larger than 4, showing good deformation capacity. Compared with the reinforced concrete shear walls, the LSLC shear walls show better deformation capacity.

(3) The equivalent damping ratio (h_{eq}) of the LSLC shear wall is calculated the values of 12~20%. Compared with the reinforced concrete shear walls, the LSLC shear walls show lower energy absorption capacity.

6. Acknowledgements

The financial support of the Self-funded Project of China Academy of Building Research Co., Ltd (for Applied Technology Research, Grant No. 20151802330730055) is gratefully appreciated.

7. References

[1] Nithyadharan, M. and V. Kalyanaraman, Behaviour of cold-formed steel shear wall panels under monotonic and reversed cyclic loading. Thin-Walled Structures 2012; 60: 12-23.

[2] Balh, N., et al., Design of steel sheathed cold-formed steel framed shear walls. Thin-Walled Structures 2014; 75: 76-86.

[3] Yu, C., Shear resistance of cold-formed steel framed shear walls with 0.686 mm, 0.762 mm, and 0.838 mm steel sheet sheathing. Engineering Structures 2010; 32(6): 1522-1529.

[4] Moghimi, H. and H.R. Ronagh, Performance of light-gauge cold-formed steel strap-braced stud walls subjected to cyclic loading. Engineering Structures 2009; 31(1): 69-83.

[5] Institute, A.I.A.S., North American standard for cold-formed steel framing-lateral design. AISI S213, USA; 2007.

[6] EN, Eurocode3: Design of steel structures-part 1-3: general rules-supplementary rules for cold-formed members and sheeting, European Committee for Standardization; 2006.

[7] Ramamurthy, K., E.K. Kunhanandan Nambiar and G. Indu Siva Ranjani, A classification of studies on properties of foam concrete. Cement and Concrete Composites 2009; 31(6): 388-396.

[8] Flores-Johnson, E.A. and Q.M. Li, Structural behaviour of composite sandwich panels with plain and fibre-reinforced foamed concrete cores and corrugated steel faces. Composite Structures 2012; 94(5): 1555-1563.

[9] Othuman Mydin, M.A. and Y.C. Wang, Structural performance of lightweight steel-foamed concrete–steel composite walling system under compression. Thin-Walled Structures 2011; 49(1): 66-76.

[10] Jones, M.R. and A. McCarthy, Preliminary views on the potential of foamed concrete as a structural material. Magazine of Concrete Research 2005; 57: 21-31(10).

[11] Mydin, M.A.O. and Y.C. Wang, Mechanical properties of foamed concrete exposed to high temperatures. Construction and Building Materials 2012; 26(1): 638-654.

[12] Ministry of housing and urban-rural development. Technical specification of lightweight steel and lightweight concrete structure (draft for examination). 2014 [in Chinese].

[13] GB/T2518-2008. Continuously hot-dip zinc-coated steel sheet and strip. Beijing: Standards Press of China 2009 [in Chinese].

[14] Iso15481-1999. Cross recessed pan head drilling screws with tapping screw thread. International Standards Organization 1999.

[15] GB/T50080-2002. Standard for test method of performance on ordinary fresh concrete. Beijing: Architecture Industrial Press of China 2003 [in Chinese].

[16] T. Shimazu, Y. Fukuhara, T. Satoh, K. Ohta, New reinforced concrete structure, 2002 [in Japanese].

[17] H. Tomatsuri, Seismic response characteristic for shear walls with high isolated structural system, Proceedings of the Japan Concrete Institute, vol.31, No.2, pp.409-414, 2009 [in Japanese].

